



**University of
Zurich**^{UZH}

**Zurich Open Repository and
Archive**

University of Zurich
University Library
Strickhofstrasse 39
CH-8057 Zurich
www.zora.uzh.ch

Year: 2014

**Water deficit induces chlorophyll degradation via the 'PAO/phyllobilin'
pathway in leaves of homoio- (*Craterostigma pumilum*) and
poikilochlorophyllous (*Xerophyta viscosa*) resurrection plants**

Christ, Bastien ; Egert, Aurélie ; Süssenbacher, Iris ; Kräutler, Bernhard ; Bartels, Dorothea ; Peters, Shaun ; Hörtensteiner, Stefan

Abstract: Angiosperm resurrection plants exhibit poikilo- or homoiochlorophylly as a response to water deficit. Both strategies are generally considered as effective mechanisms to reduce oxidative stress associated with photosynthetic activity under water deficiency. The mechanism of water deficit-induced chlorophyll (Chl) degradation in resurrection plants is unknown but has previously been suggested to occur as a result of non-enzymatic photooxidation. We investigated Chl degradation during dehydration in both poikilochlorophyllous (*Xerophyta viscosa*) and homoiochlorophyllous (*Craterostigma pumilum*) species. We demonstrate an increase in the abundance of PHEOPHORBIDE a OXYGENASE (PAO), a key enzyme of Chl breakdown, together with an accumulation of phyllobilins, that is, products of PAO-dependent Chl breakdown, in both species. Phyllobilins and PAO levels diminished again in leaves from rehydrated plants. We conclude that water deficit-induced poikilochlorophylly occurs via the well-characterized PAO/phyllobilin pathway of Chl breakdown and that this mechanism also appears conserved in a resurrection species displaying homoiochlorophylly. The roles of the PAO/phyllobilin pathway during different plant developmental processes that involve Chl breakdown, such as leaf senescence and desiccation, fruit ripening and seed maturation, are discussed.

DOI: <https://doi.org/10.1111/pce.12308>

Posted at the Zurich Open Repository and Archive, University of Zurich

ZORA URL: <https://doi.org/10.5167/uzh-104517>

Journal Article

Accepted Version

Originally published at:

Christ, Bastien; Egert, Aurélie; Süssenbacher, Iris; Kräutler, Bernhard; Bartels, Dorothea; Peters, Shaun; Hörtensteiner, Stefan (2014). Water deficit induces chlorophyll degradation via the 'PAO/phyllobilin' pathway in leaves of homoio- (*Craterostigma pumilum*) and poikilochlorophyllous (*Xerophyta viscosa*) resurrection plants. *Plant, Cell Environment*, 37(11):2521-2531.

DOI: <https://doi.org/10.1111/pce.12308>

1 Water deficit induces chlorophyll degradation via the “PAO/phyllobilin” pathway in leaves of
2 homoio- (*Craterostigma pumilum*) and poikilochlorophyllous (*Xerophyta viscosa*)
3 resurrection plants

4
5 Running title: Chlorophyll breakdown in resurrection plants

6
7 Bastien Christ¹, Aurélie Egert^{*1}, Iris Süssenbacher^{*2}, Bernhard Kräutler², Dorothea Bartels³, Shaun
8 Peters^{#4} and Stefan Hörtensteiner^{#1}

9
10 ¹Institute of Plant Biology, Molecular Plant Physiology, University of Zürich, Zollikerstrasse 107,
11 CH-8008 Zürich, Switzerland

12 ²Institute of Organic Chemistry and Center for Molecular Biosciences, University of Innsbruck,
13 Innrain 80/82, A-6020 Innsbruck, Austria

14 ³Institute of Molecular Physiology and Biotechnology of Plants, University of Bonn, Kirschallee 1, D-
15 53115 Bonn, Germany

16 ⁴Institute for Plant Biotechnology, Department of Genetics, University of Stellenbosch, Private Bag
17 X1, Matieland, 7602, South Africa

18
19 ^{*}These authors have equally contributed to the paper

20 [#]Co-last authors

21
22
23
24
25
26 Author for correspondence:

27

28 Stefan Hörtensteiner
29 Institute of Plant Biology
30 University of Zurich
31 Zollikerstrasse 107
32 CH-8008 Zurich
33 Switzerland
34
35 FAX: +41 44 634 82 04
36 email: shorten@botinst.uzh.ch
37

38 **ABSTRACT**

39 Angiosperm resurrection plants exhibit poikilo- or homoiochlorophylly as a response to water deficit.
40 Both strategies are generally considered as effective mechanisms to reduce oxidative stress associated
41 with photosynthetic activity under water deficiency. The mechanism of water deficit-induced Chl
42 degradation in resurrection plants is unknown but has previously been suggested to occur as a result of
43 nonenzymatic photooxidation. We investigated Chl degradation during dehydration in both
44 poikilochlorophyllous (*Xerophyta viscosa*) and homoiochlorophyllous (*Craterostigma pumilum*)
45 species. We demonstrate an increase in the abundance of PHEOPHORBIDE *a* OXYGENASE (PAO),
46 a key enzyme of Chl breakdown, together with an accumulation of phyllobilins, i.e. products of PAO-
47 dependent Chl breakdown, in both species. Phyllobilins and PAO levels diminished again in leaves
48 from rehydrated plants. We conclude that water-deficit induced poikilochlorophylly occurs via the
49 well characterized PAO/phyllobilin pathway of Chl breakdown and that this mechanism also appears
50 conserved in a resurrection species displaying homoiochlorophylly. The role(s) of the PAO/phyllobilin
51 pathway during different plant developmental processes that involve Chl breakdown, such as leaf
52 senescence and desiccation, fruit ripening and seed maturation, are discussed.

53

54

55 **KEYWORDS**

56 chlorophyll breakdown, *Craterostigma pumilum*, desiccation tolerance, homoiochlorophyllous,
57 PAO/phyllobilin pathway, phyllobilins, poikilochlorophyllous, resurrection plants, *Xerophyta viscosa*

58

INTRODUCTION

In contrast to the majority of plants, resurrection or desiccation-tolerant plants are characterized by their ability to tolerate and survive extreme desiccation, withstanding the loss of up to 90-95% of the cellular water in their vegetative tissues and resuming normal metabolism within a short period after rehydration (Gaff & McGregor 1979; Farrant 2000; Scott 2000; Proctor & Tuba 2002; Vitré, Farrant & Driouich 2004). Desiccation tolerance entails cellular, biochemical, and molecular changes during dehydration (Vitré *et al.* 2004), including the synthesis of (i) carbohydrates (Whittaker *et al.* 2001; Peters *et al.*, 2007; Toldi, Tuba & Scott 2009), (ii) intrinsically disordered proteins such as late embryogenesis-abundant proteins and small heat shock proteins (Ingram & Bartels 1996), (iii) antioxidants (Kranter *et al.* 2002; Mowla *et al.* 2002; Vitré *et al.* 2004) and, (iv) volatile and non-volatile isoprenoids (Beckett *et al.* 2012).

Resurrection plants are grouped into two categories regarding chlorophyll (Chl): homoiochlorophyllous and poikilochlorophyllous plants. Homoiochlorophyllous species retain most or all Chl during drying and preserve their photosynthetic apparatus, while poikilochlorophyllous species lose most of their Chl and dismantle the photosynthetic apparatus during dehydration (Tuba *et al.* 1994; Sherwin & Farrant 1996; Tuba, Proctor & Csintalan 1998). Parallel to the loss of Chl, chloroplasts of the poikilochlorophyllous genera *Xerophyta* show grana dismantling, thylakoid vesiculation, and cessation of photosynthetic CO₂ assimilation and respiration (Gaff & McGregor 1979; Tuba *et al.* 1996; Collett *et al.* 2003; Ingle *et al.* 2008). Chl breakdown during desiccation seems to be related to protection against oxidative damage caused by overreduction of the electron transport chain (Farrant 2000). This hypothesis is supported by the observation that *Xerophyta scabrifolia* preserves most of the Chl when dried in the dark, but degrades Chl during desiccation under day/night growth conditions (Tuba *et al.* 1996). Upon rehydration, photochemical activity recovers rapidly in *Xerophyta* species (Farrant 2000). Transition of desiccoplasts, i.e. plastids of dehydrated poikilochlorophyllous leaves (also termed xeroplasts in *Xerophyta* species) to photosynthetically active chloroplasts implies formation of grana, Chl biosynthesis, and light-dependent restoration of photosystem (PS) II (PSII) photochemistry and CO₂ assimilation (Ingle *et al.* 2008; Pérez *et al.* 2011; Solymosi, Tuba & Böddi 2013).

By contrast, during desiccation in homoiochlorophyllous plants (like the genera *Craterostigma*), chloroplasts adopt an oval shape and partially lose their internal organization with grana stacks largely preserved (Schneider *et al.* 1993). Active protection mechanisms of chloroplasts in homoiochlorophyllous plants also include the transient accumulation of plastid-localized stress proteins (Schneider *et al.* 1993; Gechev *et al.* 2012). It has been argued that a combination of physical (inward curling of leaves) and chemical (increase in anthocyanin content and antioxidative enzyme activities) mechanisms enable protection against potential photooxidative damage resulting from Chl excitation in dry leaves (Sherwin & Farrant 1998).

To date, the mechanism of Chl degradation during desiccation in resurrection plants is unknown. In poikilochlorophyllous species, Chl degradation has been suggested to be the result of photooxidation rather than of enzymatic processes (Tuba *et al.* 1996; Proctor & Tuba 2002). Here, we investigated whether Chl degradation during desiccation in the poikilochlorophyllous species *Xerophyta viscosa* (*X. viscosa*) and the homoiochlorophyllous species *Craterostigma pumilum* (*C. pumilum*) follows the well-described “PAO/phyllobilin pathway”, shown to be active during leaf senescence and fruit ripening of higher plants (reviewed in Kräutler 2008; Hörtensteiner & Kräutler 2011; Christ & Hörtensteiner 2013; Kräutler & Hörtensteiner 2013). In this pathway (Fig. 1), Chl is ultimately broken down to a group of linear tetrapyrroles, termed phyllobilins (Kräutler & Hörtensteiner 2013). The major classes of phyllobilins identified from different species can be categorized into formylxobilin-type nonfluorescent Chl catabolites (NCCs) (Kräutler & Matile 1999) and dioxobilin-type nonfluorescent Chl catabolites (DNCCs) (Christ *et al.* 2013; Süssbacher *et al.* 2014; Kräutler & Hörtensteiner 2013). The structural relation of these phyllobilins is based on the activity of PHEOPHORBIDE *a* OXYGENASE (PAO), a key enzyme of the pathway (Hörtensteiner *et al.* 1998), which together with RED CHLOROPHYLL CATABOLITE REDUCTASE (RCCR) (Rodoni *et al.* 1997) catalyzes the oxygenolytic porphyrin ring opening of pheophorbide *a*, a phytol- and Mg-free intermediate of breakdown, yielding a *primary* fluorescent Chl catabolite (*pFCC*) (Mühlecker *et al.* 1997; Pružinská *et al.* 2007) or its epimer, *epi-pFCC* (Mühlecker *et al.* 2000) (Fig. 1). It was recently shown in *Arabidopsis thaliana* that protein-protein interaction between the chloroplast-localized enzymes of the PAO/phyllobilin pathway allows metabolite channeling between

Chl and *p*FCC and, thus, controlled degradation of potentially phototoxic Chl catabolites (Sakuraba *et al.* 2012; Sakuraba *et al.* 2013). *p*FCC, considered to be the first non-phototoxic Chl catabolite, is exported from the chloroplast (Hörtensteiner 2006). Subsequently, modified fluorescent Chl catabolites are formed in the cytosol by species-specific functionalization of *p*FCC at different peripheral side groups. After import into the vacuole, these fluorescent compounds are converted to respective NCCs through isomerization catalyzed by the acidic vacuolar pH (Oberhuber *et al.* 2003; Kräutler & Hörtensteiner 2013). NCCs have been shown to be prone to further oxidation (Ulrich *et al.* 2011) yielding yellow Chl catabolites (YCCs). Chemical oxidation of NCCs to YCCs has been demonstrated in vitro, however, YCCs were also found in extracts of fresh senescent leaves of *Cercidiphyllum japonicum*, indicating that they may also be formed in vivo (Moser *et al.* 2008; Ulrich *et al.* 2011; Scherl, Müller & Kräutler 2012) (Fig. 1).

To date, Chl catabolites (Kräutler 2008; Kräutler & Hörtensteiner 2013) and breakdown mechanisms have largely been described during senescence processes, which ultimately lead to the death of respective tissues (Hörtensteiner 2006; Hörtensteiner & Kräutler 2011). Here, we provide evidence that Chl breakdown during desiccation of the poikilochlorophyllous resurrection plant *X. viscosa* is mediated by the PAO/phyllobilin pathway (Kräutler & Hörtensteiner 2013). Thus, like during leaf senescence (Pružinská *et al.* 2005), PAO is up-regulated and several NCCs accumulate during the drying phase in *X. viscosa* leaves. Upon rehydration, NCC abundance decreases in regreening leaves. In addition, our study indicates that Chl breakdown also follows the PAO/phyllobilin pathway and abundance of Chl catabolites decrease during rehydration in the homoiochlorophyllous species *C. pumilum*. However, compared to *X. viscosa*, significant amounts of YCCs accumulate, indicating higher oxidative damage in the homoiochlorophyllous species.

MATERIALS AND METHODS

Plant material

X. viscosa and *C. pumilum* plants were propagated under greenhouse conditions as previously described (Bartels *et al.* 1990; Peters *et al.* 2007). Plants used for water deficit experiments were

grown in a controlled-environment chamber (*X. viscosa*, 16 h light with 130 $\mu\text{mol photons m}^{-2} \text{ s}^{-1}$ / 8 h dark, 25°C, 60% relative humidity; *C. pumilum*, 14 h light with 180 $\mu\text{mol photons m}^{-2} \text{ s}^{-1}$, 24°C / 10 h dark, 20°C, 60% relative humidity).

Water deficit stress treatment

Water deficit stress was imposed on whole potted plants by withholding irrigation at the end of which the relative water content (RWC) was determined to be 5-10%. Leaf samples were excised at regular intervals, immediately flash-frozen in liquid nitrogen, ground, freeze-dried and stored at -80°C. Sampling times were determined by visual appraisal of the plants using leaf decoloration and folding as benchmarks, at which times the RWC of leaves was determined as previously described (Barrs & Weatherley 1962; Peters *et al.* 2007). Rehydration was conducted by watering the plants and sampling as described above. For *C. pumilum*, “non-senescent” (surviving) and “senescent” (yellowing and dying) leaf samples were collected separately at four different time points [“hydrated” (RWC: ~80-95%), “partially dehydrated” (RWC: ~30-40%), “dried” (RWC: ~5-10%) and “rehydrated” (RWC: ~80-95%)]. Images of leaf sections (*X. viscosa*) or whole plants (*C. pumilum*) were captured with a digital camera at each sampling time point.

Analysis of chlorophyll and chlorophyll catabolites

Chl was extracted from freeze-dried samples in 80% acetone and supernatants were analyzed spectrophotometrically (Strain, Cope and Svec 1971). Phyllobilins were extracted and analyzed by HPLC (setup “1”) as previously described (Christ *et al.* 2012), except that freeze-dried samples were homogenized with 18 volumes (w/v; *X. viscosa*) or 50 volumes (w/v; *C. pumilum*) of 50 mM phosphate buffer, pH 7:methanol (1:3, v/v). Co-injection analysis was performed using another HPLC system [setup “2” (Scherl *et al.* 2012); Dionex UltiMate 3000 system (pump and diode array detector)] equipped with a C18 ODS column (5 μm , 250 x 4.6 mm, Phenomenex), which was developed with a gradient (flow rate 0.5 mL min^{-1}) of solvent B (100% methanol) in solvent A (10 mM ammonium acetate buffer, pH 7.0) as follows: 38% during 2 min, 38% to 64% in 27 min, 64% to 100% in 3 min

and 100% during 3 min. *Zm*-NCC-2 was prepared from senescent *Z. mays* leaves as described (Berghold *et al.* 2006).

For MS analysis, a *Xv*-NCC-3-containing fraction was isolated by HPLC using setup “2” (see above), which had the following spectroscopic characteristics: UV/Vis: λ_{\max} = 315 nm. Circular dichroism (CD; $c = 3.9 \cdot 10^{-5}$ M): $\lambda_{\min/\max}$ [nm] ($\Delta\epsilon$) = 316 (4.5), 281 (-4.1), 251 sh (-1.4), 224 (4.9). The sample of *Xv*-NCC-3 was further analyzed by electro-spray ionization mass spectrometry (ESI-MS; Finnigan LCQ classic, positive ion mode, spray voltage 4.25 kV): m/z (% intensity) = 883.2 (14, [M-H+2K]⁺); 867.2 (12, [M-H+Na+K]⁺); 845.2 (77, [M+K]⁺); 829.3 (41, [M+Na]⁺); 809.2 (12), 808.2 (44), 807.2 (100, C₄₁H₅₁N₄O₁₃⁺, [M+H]⁺); 775.3 (33, [M-CH₄O+H]⁺); 684.2 (21, [M-C₇H₉NO (ring A)+H]⁺); 652.3 (7, [M-ring A-CH₄O+H]⁺); 645.2 (18, [M-C₆H₁₀O₅ (glucose)+H]⁺); 613.2 (13, [M-CH₄O-glucose+H]⁺).

Protein extraction and immunoblot analysis

Total leaf proteins were prepared as described (Ingle, Smith & Sweetlove 2005) with the following modifications. Total proteins were isolated from freeze-dried samples by homogenization in 15 volumes (w/v; *X. viscosa*) or 25 volumes (w/v; *C. pumilum*) of ice-cold extraction buffer [0.5 M Tris-HCl, pH 7.5, 10 mM EDTA, 1% (v/v) Triton X-100, 2% (v/v) 2-mercaptoethanol] complemented with a protease inhibitor cocktail (Complete; Roche Applied Science). Samples were centrifuged at 12'000g for 5 min and protein concentration of the supernatant determined using the Bradford Assay (Bio-Rad). Proteins were subsequently precipitated with chloroform-methanol (Wessel & Flügge 1984) and analyzed by SDS-PAGE and immunoblotting as described (Pružinská *et al.* 2007; Schelbert *et al.* 2009). SDS-PAGE gels were loaded with proteins extracted from equal amounts of dry weight. The following antibodies were used for immunoblot analysis: polyclonal antibodies against LHCb1 and PsbA (1:2000; AgriSera) and monoclonal (*X. viscosa*; 1:500) or polyclonal (*C. pumilum*; 1:2000) antibodies against PAO (kindly provided by Prof. John Gray, University of Toledo; Gray *et al.* 2004).

RESULTS

Relative water content, chlorophyll content and leaf morphology

X. viscosa plants were dehydrated by withholding irrigation. Leaf RWC consequently dropped to below 10% within 15 d (Fig. 2A). Following 7 d in the desiccated state, plants were irrigated. During this rehydration period, leaf RWC increased rapidly and full turgor was reached after 3 d. Chl was gradually degraded during the dehydration period leading to almost Chl-free dehydrated leaves (Fig. 2B). During rehydration, Chl biosynthesis was rapidly induced and concentrations reached 75% of those observed in leaves prior to the water deficit (full turgor, unstressed) within 10 d. Because of the water and Chl loss, leaf morphology changed dramatically during the dehydration and rehydration period (Fig. 2C). Leaves folded along their midribs and changed color from green to yellow due to Chl degradation and unmasking of other leaf pigments. During the recovery period, rehydration preceded Chl resynthesis, and therefore fully rehydrated leaves exhibited a transition phase between yellow and green color.

Under comparable dehydration conditions, not all leaves of *C. pumilum* responded consistently (Fig. 3). The youngest leaves (“non-senescent”) shrunk and turned green-purple due to the loss of water and the accumulation of anthocyanins, as previously reported (Farrant 2000). In contrast, the oldest leaves (“senescent”) changed color from green to yellow and did not shrink as much as “non-senescent” leaves (Fig. 3C). These visual observations corroborated changes in Chl concentrations, which did not significantly change in “non-senescent” leaves but dramatically decreased in “senescent” leaves during dehydration (Fig. 3B). During rehydration, “non-senescent” leaves recovered full turgor (increase of RWC from 5% to 90%, Fig. 3A) and Chl concentrations comparable to those observed in leaves prior to the water deficit (full turgor, unstressed, Fig. 3B) whereas “senescent” leaves did not recover and died.

PAO abundance increases during dehydration in *X. viscosa* and *C. pumilum* leaves

Total protein profiles of *X. viscosa* leaves were investigated during dehydration and rehydration by SDS-PAGE and Coomassie blue staining (Fig. 4A). The total protein concentration ($\mu\text{g mg}^{-1}$ DW) did not change significantly during dehydration and, therefore, for each sample the same amount of protein (fifteen microgram) was loaded on SDS-PAGE gels. Levels of large and small subunits of

Rubisco, indicated with black arrowheads in Fig. 4A, stayed rather constant. However, immunoblot analysis revealed changes of the levels of thylakoid proteins involved in photosynthesis as previously reported for poikilochlorophyllous *Xerophyta* species (Fig. 4B; Collett *et al.* 2003; Collett *et al.* 2004; Ingle *et al.* 2007; Ingle *et al.* 2008; Pérez *et al.* 2011). Indeed, PsbA, a subunit of the core complex of PSII, was quantitatively degraded during dehydration and resynthesized during rehydration, similarly to Chl. The same pattern was observed for LHCb1, a component of the light-harvesting antennae of PSII.

To investigate whether Chl is broken down through the well-described PAO/phyllobilin pathway, PAO protein levels were investigated during dehydration and rehydration (Fig. 4B). PAO abundance increased during dehydration, but decreased during rehydration; i.e. it was negatively correlated with the concentration of Chl. Surprisingly, the PAO abundance was highest after 1 d of rehydration.

In contrast to *X. viscosa* in *C. pumilum* leaves, large proportions of proteins were degraded during dehydration and resynthesized during rehydration (Fig. 4C; Bernacchia, Salamini & Bartels 1996). Indeed, protein content decreased by 50% in “non-senescent” leaves and by more than 95% in “senescent” leaves. Therefore, SDS-PAGE gels were loaded based on equal amounts of plant material (dry weight; five milligrams). Abundance of the large and small subunits of Rubisco (indicated with black arrowheads in Fig. 4C) as well as photosystem components such as PsbA and LHCb1 (Fig. 4D) decreased dramatically in “senescent” leaves. Furthermore, Rubisco and photosystem subunits appeared to be partially degraded in “non-senescent” leaves (Fig. 4C and D), which is in agreement with transcript accumulation patterns (Bernacchia *et al.* 1996). PAO abundance increased in both “senescent” and “non-senescent” leaves, suggesting that chlorophyll degradation occurs in the entire plant during desiccation (Fig. 4D).

Leaves of *X. viscosa* and *C. pumilum* accumulate phyllobilins during dehydration

The water deficit-induced increase in PAO abundance in leaves of *X. viscosa* points to a possible involvement of the PAO/phyllobilin pathway in the breakdown of Chl. PAO is a key enzyme of the pathway because it opens the macrocycle of pheophorbide *a* and therefore determines the basic structure of all downstream linear catabolites (phyllobilins; Kräutler & Hörtensteiner 2013). In order

to investigate the presence of such catabolites, samples were collected at different time points during dehydration and rehydration and analyzed by reversed-phase HPLC (Fig. 5A). Spectral analysis of the resulting chromatograms allowed the identification of four fractions, tentatively named *Xv*-NCC-1 to -4, showing typical NCC absorbance properties (Fig. 5B, Supplemental Fig. S1; Kräutler & Hörtensteiner 2013). These fractions were absent prior to dehydration and increasingly accumulated in the leaves during dehydration and Chl degradation. After 10 d of subsequent rehydration, they had almost completely disappeared. In-depth analysis of the major fraction, *Xv*-NCC-3, by mass spectrometry revealed that this NCC has the same mass (m/z $[M+H^+] = 807.2$; Fig. 5B) as *Zm*-NCC-2, an NCC described from *Zea mays* (Berghold *et al.* 2006). HPLC analysis of purified fractions showed that *Xv*-NCC-3 and *Zm*-NCC-2 exhibited the same retention time when analyzed independently and co-eluted as a single fraction when co-injected as a 1:1 (w/w) mixture (Fig. 5C). This observation indicates that *Xv*-NCC-3 has the same structure as *Zm*-NCC-2 (Fig. 5D; Berghold *et al.* 2006). *Xv*-NCC-3/*Zm*-NCC-2 carries a methyl ester group at C13² position (see Fig. 1) indicating the likely absence in *X. viscosa* of a homolog of METHYLESTERASE16, responsible for the ester hydrolysis in *A. thaliana* (Christ *et al.* 2012). The C8²-ethyl moiety of *Xv*-NCC-3 is hydroxylated and subsequently glycosylated (see Fig. 5D); respective modifications are also known to occur in natural NCCs from e.g. *A. thaliana*, *Brassica napus*, *Nicotiana rustica*, *Pyrus communis* and *Z. mays* (Kräutler & Hörtensteiner 2013). The structural identity of *Xv*-NCC-3 with *Zm*-NCC-2 also implied the same stereoselectivity of the respective RCCRs from *X. viscosa* and *Z. mays* (Berghold *et al.* 2006). RCCR reduces red Chl catabolite (RCC) produced by PAO to *p*FCC (Pružinská *et al.* 2005; Pružinská *et al.* 2007). Depending on the plant species, RCCRs exhibit different stereospecificities in the reduction of the C20/C1 (see Figs. 1 and 5D) double bond of RCC and therefore yield one of the two possible C1-stereoisomers, i.e. *p*FCC or *epi-p*FCC (Moser *et al.* 2009; Kräutler & Hörtensteiner 2013). From the identity of *Xv*-NCC-3 and *Zm*-NCC-2, the C1 stereochemistry of *X. viscosa* RCCR can be deduced: it yields *epi-p*FCC like the RCCRs from *Z. mays*, *N. rustica*, *Spinacia oleracea* and *Cercidiphyllum japonicum* (Kräutler & Hörtensteiner 2013).

Like observed for *X. viscosa*, dehydration of *C. pumilum* also led to the accumulation of Chl catabolites in leaves (Fig. 6A and B). In “senescent” leaves, in which the Chl content decreased

dramatically during desiccation (Fig. 3B), several NCCs and YCCs were found and were classified on the basis of their characteristic UV/Vis spectra (Fig. 6A, Supplemental Fig. S1; see Moser *et al.* 2008; Ulrich *et al.* 2011). However, phyllobilins were also identified in “non-senescent” leaves, indicating that Chl is also partially degraded in these leaves, although the decrease in Chl content was not significant when determining Chl concentrations at the different sampling times (Fig. 3B). The accumulation of NCCs and YCCs (Fig. 6A and B), together with the increase in PAO abundance (Fig. 4D), suggests that water deficit-induced Chl breakdown also occurs in *C. pumilum* and is mediated enzymatically by the PAO/phyllobilin pathway. During rehydration of “non-senescent” leaves, colorless Chl catabolites disappeared rapidly (Fig. 6A and B), comparable to the observation in *X. viscosa* (Fig. 5A).

DISCUSSION

The ultimate fate of a senescing leaf is death; however, leaf senescence can be considered to be reversible until a “point of no return”, indicating that the processes of leaf senescence themselves take place in living tissue (Thomas *et al.* 2003; Thomas 2013). Indeed, chloroplast-to-gerontoplast (senescent chloroplast) transition has been shown to be reversible in *N. rustica* (Zavaleta-Mancera *et al.* 1999a; Zavaleta-Mancera *et al.* 1999b). Shoot decapitation of senescing *N. rustica* plants leads to leaf regreening, an effect that is enhanced by treatment with cytokinins, which are known to inhibit senescence (Gan & Amasino 1997). Leaf regreening was shown to involve resynthesis of functional thylakoid membranes within gerontoplasts rather than *de novo* formation of chloroplasts (Zavaleta-Mancera *et al.* 1999a, b).

In this study, we focused on the well characterised leaf de- and regreening associated with Chl breakdown in poikilochlorophyllous resurrection plants (Tuba *et al.* 1996; Sherwin & Farrant 1998; Farrant 2000), focusing on *X. viscosa*. We hypothesized that similar reversible mechanisms of chloroplast dismantling are shared between age-dependent leaf senescence of higher plants and leaf dehydration of poikilochlorophyllous plants. Although, the process of poikilochlorophylly (complete loss of Chl during desiccation of resurrection plants) has been well described (Tuba *et al.* 1994;

Sherwin & Farrant 1996; Tuba *et al.* 1998), Chl breakdown has been speculated to occur via nonenzymatic photooxidation events (Tuba *et al.* 1996; Proctor & Tuba 2002). Likewise, senescence processes of resurrection plants, including Chl breakdown, are poorly understood (Denev, Stefanov & Terashima 2012) and an involvement of the PAO/phyllobilin pathway has not been demonstrated. Here, we provide evidence that during dehydration of *X. viscosa* Chl is degraded enzymatically via the PAO/phyllobilin pathway (Kräutler & Hörtensteiner 2013) to various NCCs (Fig. 5), the major one (*Xv*-NCC-3) being identical to *Zm*-NCC-2 of maize (Berghold *et al.* 2006). Although we were unable to precisely quantify the amounts of phyllobilins during desiccation, leaving open the possibility that a minor fraction of Chl may be degraded non-enzymatically, the increases in phyllobilin and PAO abundance during dehydration (Fig. 4B), suggest that water deficit-induced poikilochlorophyllly in *X. viscosa* leaves is mechanistically comparable to the highly regulated PAO/phyllobilin pathway active during leaf senescence and fruit ripening (Kräutler & Hörtensteiner 2013).

A major function of Chl breakdown in leaves and fruits is the detoxification of photoactive Chl and breakdown intermediates, thereby increasing cell viability during senescence. Indeed, suppression of PAO results in a premature cell death phenotype, which is caused by the accumulation of phototoxic pheophorbide *a* (Pružinská *et al.* 2003; Tanaka *et al.* 2003). As a consequence, respective mutants such as *A. thaliana paol* and *Z. mays lls1* exhibit severe defects in growth, senescence and fertility (Gray *et al.* 1997; Pružinská *et al.* 2005). Similarly, it has been argued that Chl degradation in poikilochlorophyllous resurrection plants is a strategy to avoid photooxidative damage caused by Chl in dry leaves, and, thus, enhances plant survival during and after dehydration (Proctor & Tuba 2002). It is tempting to speculate that in poikilochlorophyllous species mutations of components of the PAO/phyllobilin pathway, which during senescence of desiccation-intolerant plants causes the retention of Chl within Chl-apoprotein complexes and/or the accumulation of photodynamic breakdown intermediates (Pružinská *et al.* 2005; Park *et al.* 2007; Pružinská *et al.* 2007; Hörtensteiner 2009), would cause photooxidative damage during desiccation, and, thus, would dramatically decrease the resurrection capacity of these plants.

By contrast, homoiochlorophyllous resurrection species retain large proportions of Chl during desiccation. Such plants have developed other protection mechanisms such as leaf curling which, apart

from chemical protection mechanisms, has an important light shading effect on Chl-apoprotein complexes (Farrant *et al.* 2003). Nevertheless, homoiochlorophyllous species also degrade (some) Chl during desiccation (Farrant *et al.* 1999; Alamillo & Bartels 2001). We could demonstrate that a comparable enzymatic mechanism of Chl breakdown (i.e. the PAO/phyllobilin pathway) is also active in the leaves of *C. pumilum*. A major difference was found in the type of phyllobilins that accumulate during dehydration. The specific occurrence of YCCs, i.e. oxidation products of NCCs that may be formed in vivo (Moser *et al.* 2008; Ulrich *et al.* 2011, Kräutler & Hörtensteiner 2013) in *C. pumilum* leaves suggests increased oxidative stress potential in this homoiochlorophyllous species. Interestingly, YCC accumulation was not limited to the surviving leaves (“non-senescent”) of the plant, but also occurred in leaves that did not recover from dehydration (“senescent”). This finding may indicate that, during dehydration, leaves of homoiochlorophyllous species are subjected to more severe oxidative stress compared to those of poikilochlorophyllous species, presumably due to the higher concentrations of Chl present in the former. In line with this, homoiochlorophyllous species have been shown to accumulate large amounts of malondialdehyde during desiccation (Djilianov *et al.* 2011; Jovanovic *et al.* 2011). Malondialdehyde is a breakdown product of lipid peroxidation and, thus, an indicator of cellular oxidative damage.

For many desiccation-intolerant species phyllobilins have been shown to progressively accumulate in the vacuole during senescence and to persist until the leaf dies or sheds (Kräutler & Hörtensteiner 2013). Interestingly, in both *X. viscosa* and *C. pumilum*, rehydration was accompanied by the disappearance of accumulated phyllobilins. The mechanism of this phenomenon remains unknown, but likely occurs through further degradation of the tetrapyrrole backbone of the phyllobilins. In both homoio- and poikilochlorophyllous species, the central vacuole is fragmented to small vacuoles during dehydration and re-formation of the large central vacuole (during rehydration) is thought to occur by fusion of these smaller ones (Rascio & Rocca 2005). Thus, we assume that phyllobilin degradation should occur during this vacuolar merging phase.

Parallel to Chl breakdown, PS core and antennae subunits are also degraded during dehydration of *X. viscosa* (Fig. 4B). Both Chl biosynthesis and degradation are known to be linked with PS assembly and disassembly, because Chl molecules are intimately integrated within PS subunits

(Nelson & Yocum 2006; Hörtensteiner 2009; Tanaka & Tanaka 2011). Consequently, suppression of genes involved in the early steps of the PAO/phyllobilin pathway inhibits the degradation of several PS components, in particular LHCII subunits (Park *et al.* 2007; Schelbert *et al.* 2009). In addition to its detoxifying role, Chl degradation during leaf senescence is thought to be a prerequisite for the degradation and remobilization of PS proteins, which contain a significant fraction of nitrogen present in mesophyll cells (Hörtensteiner & Feller 2002). From this perspective, the correlation between the degradation of Chl and Chl-binding proteins observed in both the homoio- and poikilochlorophyllous species is not overly surprising. By contrast, however, Rubisco was not degraded during dehydration of *X. viscosa* (Fig. 3A), pointing to a major difference between leaf desiccation and senescence. Previous observations have noted that the mechanisms of chloroplast dismantling during dehydration of poikilochlorophyllous plants differs from leaf senescence (Proctor & Tuba 2002) and that senescence reduces desiccation tolerance (Gaff 1986). During leaf senescence, Rubisco, which accounts for 20–30% of total leaf nitrogen, is also degraded for nitrogen remobilization (Feller, Anders & Mae 2008). It is most likely that nitrogen remobilization is irrelevant during dehydration of resurrection plants. Instead, it is reasonable to assume that the selective degradation of Chl-binding proteins during dehydration in *X. viscosa* is a prerequisite to enable Chl degradation (preventing photooxidation) with the converse being true during leaf senescence (Chl broken down as a prerequisite for nitrogen remobilization of Chl-binding proteins). In this respect, the processes occurring in *C. pumilum*, i.e. patterns of both Rubisco and PS subunit degradation correlating with Chl degradation (Fig. 4), resemble leaf senescence. It will be interesting to elucidate to what extent this assumption can be extrapolated to other aspects of senescence, for example by comparative analysis of senescence-associated gene expression in homoio- and poikilochlorophyllous species.

The finding that the PAO/phyllobilin pathway is involved during leaf desiccation in resurrection plants indicates that the same mechanism of Chl breakdown is used during leaf desiccation and leaf senescence, although the main goals of these two processes are different (survival and nutrient remobilization, respectively). Even desiccation-intolerant angiosperms exhibit desiccation tolerance, which, however, is restricted to seeds. Seed desiccation enables protection of the embryo in a dormant state until conditions are favorable for germination (Finkelstein *et al.* 2008). Seed maturation, similar

to leaf desiccation in resurrection plants (Rascio & Rocca 2005; Illing *et al.* 2005), involves the accumulation of considerable quantities of non-reducing di- and oligosaccharides, compatible solutes and specific proteins such as late embryogenesis abundant proteins and heat shock proteins (Hoekstra, Golovina & Buitink 2001). During seed maturation, the embryo degrades Chl and, interestingly, Chl degradation seems to also follow the PAO/phylobilin pathway. Thus, when *B. napus* or *A. thaliana* plants are exposed to freezing temperatures during seed maturation, seed Chl breakdown is blocked (Chung *et al.* 2006; Delmas *et al.* 2013). PAO expression was shown to be reduced under such conditions and pheophorbide *a* accumulated in frost-exposed seeds (Chung *et al.* 2006). Likewise, absence of STAY-GREEN, which is essential for Chl breakdown in senescing leaves (Hörtensteiner 2009), also causes retention of Chl during seed maturation. One famous example of mutants deficient in STAY-GREEN is Mendel's green cotyledon mutant (Armstead *et al.* 2007). The capacity of embryo degreening seems to correlate with seed storability, and germination rates of mature seeds have been demonstrated to be inversely proportional to the Chl level (Jalink *et al.* 1998). Thus, suppression of Chl *b* to *a* conversion in *A. thaliana* leads to Chl retention in the embryo during seed drying and dramatically decreases seed germination capacity (Nakajima *et al.* 2012).

In summary, we have provided evidence that both homoio- and poikilochlorophyllous plants degrade Chl via the PAO/phylobilin pathway. Our findings have extended the physiological conditions under which this pathway is active to now include the leaves of resurrection plants during dehydration. Our data support the notion that the PAO/phylobilin pathway of Chl breakdown is not restricted to conditions that ultimately lead to the death of degreening tissues, like senescing leaves and ripening fruits, but also occurs in tissues that naturally regreen at later stages, like during (epigeal) seed germination and rehydration of leaves of poikilochlorophyllous resurrection plants.

ACKNOWLEDGMENTS

We thank John Gray, University of Toledo, for antibodies against PAO. This work was supported by the Swiss National Science Foundation (grant nos. IZEBZ0_143003/1 and 31003A_132603 to S.H.) and the Austrian Science Fund (FWF, grant nos. L-472 and I-563 to B.K.).

REFERENCES

- Alamillo J.M. & Bartels D. (2001) Effects of desiccation on photosynthesis pigments and the ELIP-like dsp 22 protein complexes in the resurrection plant *Craterostigma plantagineum*. *Plant Science* **160**, 1161–1170
- Armstead I., Donnison I., Aubry S., *et al* (2007) Cross-species identification of Mendel's I locus. *Science* **315**, 73
- Barrs H. & Weatherley P. (1962) A re-examination of the relative turgidity technique for estimating water deficits in leaves. *Australian Journal of Biological Sciences* **15**, 413–428
- Bartels D., Schneider K., Terstappen G., Piatkowski D. & Salamini F. (1990) Molecular cloning of abscisic acid-modulated genes which are induced during desiccation of the resurrection plant *Craterostigma plantagineum*. *Planta* **181**, 27–34
- Beckett M., Loreto F., Velikova V., Brunetti C., Di Ferdinando M., Tattini M., Calfapietra C. & Farrant J.M. (2012) Photosynthetic limitations and volatile and non-volatile isoprenoids in the poikilochlorophyllous resurrection plant *Xerophyta humilis* during dehydration and rehydration. *Plant, Cell and Environment* **35**, 2061–2074
- Berghold J., Müller T., Ulrich M., Hörtensteiner S. & Kräutler B. (2006) Chlorophyll breakdown in maize: on the structure of two nonfluorescent chlorophyll catabolites. *Monatshefte für Chemie - Chemical Monthly* **137**, 751–763
- Bernacchia G., Salamini F. & Bartels D. (1996) Molecular characterization of the rehydration process in the resurrection plant *Craterostigma plantagineum*. *Plant Physiology* **111**, 1043–1050
- Christ B. & Hörtensteiner S. (2013) Mechanism and significance of chlorophyll breakdown. *Journal of Plant Growth Regulation* DOI 10.1007/s00344-013-9392-y
- Christ B., Schelbert S., Aubry S., Süssenbacher I., Müller T., Kräutler B. & Hörtensteiner S. (2012) MES16, a member of the methylesterase protein family, specifically demethylates fluorescent chlorophyll catabolites during chlorophyll breakdown in *Arabidopsis*. *Plant Physiology* **158**, 628–641

- 450 Christ B., Süßenbacher I., Moser S., Bichsel N., Egert A., Müller T., Kräutler B. & Hörtensteiner S.
451 (2013) Cytochrome P450 CYP89A9 is involved in the formation of major chlorophyll
452 catabolites during leaf senescence in *Arabidopsis*. *The Plant Cell* **25**, 1868–1880
- 453 Chung D.W., Pružinská A., Hörtensteiner S. & Ort D.R. (2006) The role of pheophorbide *a* oxygenase
454 expression and activity in the canola green seed problem. *Plant Physiology* **142**, 88–97
- 455 Collett H., Butowt R., Smith J., Farrant J. & Illing N. (2003) Photosynthetic genes are differentially
456 transcribed during the dehydration-rehydration cycle in the resurrection plant, *Xerophyta*
457 *humilis*. *Journal of Experimental Botany* **54**, 2593–2595
- 458 Collett H., Shen A., Gardner M., Farrant J.M., Denby K.J. & Illing N. (2004) Towards transcript
459 profiling of desiccation tolerance in *Xerophyta humilis*: construction of a normalized 11 k X.
460 *humilis* cDNA set and microarray expression analysis of 424 cDNAs in response to
461 dehydration. *Physiologia Plantarum* **122**, 39–53
- 462 Delmas F., Sankaranarayanan S., Deb S., Widdup E., Bournonville C., Bollier N., Northey J.G.B.,
463 McCourt P. & Samuel M.A. (2013) ABI3 controls embryo degreening through Mendel's *I*
464 locus. *Proceedings of the National Academy of Sciences of the United States of America* **110**,
465 E3888–E3894
- 466 Denev I., Stefanov D. & Terashima I. (2012) Preservation of integrity and activity of *Haberlea*
467 *rhodopensis* photosynthetic apparatus during prolonged light deprivation. *Physiologia*
468 *Plantarum* **146**, 121–128
- 469 Djilianov D., Ivanov S., Moyankova D., Miteva L., Kirova E., Alexieva V., Joudi M., Peshev D. &
470 Van den Ende W. (2011) Sugar ratios, glutathione redox status and phenols in the resurrection
471 species *Haberlea rhodopensis* and the closely related non-resurrection species *Chirata*
472 *eberhardtii*. *Plant Biology* **13**, 767–776
- 473 Farrant J.M. (2000) A comparison of mechanisms of desiccation tolerance among three angiosperm
474 resurrection plant species. *Plant Ecology* **151**, 29–39
- 475 Farrant J.M., Cooper K., Kruger L.A. & Sherwin H.W. (1999) The effect of drying rate on the survival
476 of three desiccation-tolerant angiosperm species. *Annals of Botany* **84**, 371–379

- 477 Farrant J.M., Vander Willigen C., Loffell D.A., Bartsch S. & Whittaker A. (2003) An investigation
478 into the role of light during desiccation of three angiosperm resurrection plants. *Plant, Cell*
479 *and Environment* **26**, 1275–1286
- 480 Feller U., Anders I. & Mae T. (2008) Rubiscolytics: fate of Rubisco after its enzymatic function in a
481 cell is terminated. *Journal of Experimental Botany* **59**, 1615–1624
- 482 Finkelstein R., Reeves W., Ariizumi T. & Steber C. (2008) Molecular aspects of seed dormancy.
483 *Annual Review of Plant Biology* **59**, 387–415
- 484 Gaff D.F. (1986) Desiccation tolerant “resurrection” grasses from Kenya and West Africa. *Oecologia*
485 **70**, 118–120
- 486 Gaff D.F. & McGregor G.R. (1979) The effect of dehydration and rehydration on the nitrogen content
487 of various fractions from resurrection plants. *Biologia Plantarum* **21**, 92–99
- 488 Gan S. & Amasino R.M. (1997) Making sense of senescence. Molecular genetic regulation and
489 manipulation of leaf senescence. *Plant Physiology* **113**, 313–319
- 490 Gechev T.S., Dinakar C., Benina M., Toneva V. & Bartels D. (2012) Molecular mechanisms of
491 desiccation tolerance in resurrection plants. *Cellular and Molecular Life Sciences* **69**, 3175–
492 3186
- 493 Gray J., Close P.S., Briggs S.P. & Johal G.S. (1997) A novel suppressor of cell death in plants
494 encoded by the *Lls1* gene of maize. *Cell* **89**, 25–31
- 495 Gray J., Wardzala E., Yang M., Reinbothe S., Haller S. & Pauli F. (2004) A small family of LLS1-
496 related non-heme oxygenases in plants with an origin amongst oxygenic photosynthesizers.
497 *Plant Molecular Biology* **54**, 39–54
- 498 Hoekstra F.A., Golovina E.A. & Buitink J. (2001) Mechanisms of plant desiccation tolerance. *Trends*
499 *in Plant Science* **6**, 431–438
- 500 Hörteneiner S. (2006) Chlorophyll degradation during senescence. *Annual Review of Plant Biology*
501 **57**, 55–77
- 502 Hörteneiner S. (2009) Stay-green regulates chlorophyll and chlorophyll-binding protein degradation
503 during senescence. *Trends in Plant Science* **14**, 155–162

- 504 Hörtensteiner S. & Feller U. (2002) Nitrogen metabolism and remobilization during senescence.
505 *Journal of Experimental Botany* **53**, 927–937
- 506 Hörtensteiner S. & Kräutler B. (2011) Chlorophyll breakdown in higher plants. *Biochimica et*
507 *Biophysica Acta* **1807**, 977–988
- 508 Hörtensteiner S., Wüthrich K.L., Matile P., Ongania K.-H. & Kräutler B. (1998) The key step in
509 chlorophyll breakdown in higher plants. Cleavage of pheophorbide *a* macrocycle by a
510 monooxygenase. *The Journal of Biological Chemistry* **273**, 15335–15339
- 511 Illing N., Denby K.J., Collett H., Shen A. & Farrant J.M. (2005) The signature of seeds in resurrection
512 plants: a molecular and physiological comparison of desiccation tolerance in seeds and
513 vegetative tissues. *Integrative and Comparative Biology* **45**, 771–787
- 514 Ingle R.A., Collett H., Cooper K., Takahashi Y., Farrant J.M. & Illing N. (2008) Chloroplast
515 biogenesis during rehydration of the resurrection plant *Xerophyta humilis*: parallels to the
516 etioplast–chloroplast transition. *Plant, Cell and Environment* **31**, 1813–1824
- 517 Ingle R.A., Schmidt U.G., Farrant J.M., Thomson J.A. & Mundree S.G. (2007) Proteomic analysis of
518 leaf proteins during dehydration of the resurrection plant *Xerophyta viscosa*. *Plant, Cell and*
519 *Environment* **30**, 435–446
- 520 Ingle R.A., Smith J.A.C. & Sweetlove L.J. (2005) Responses to nickel in the proteome of the
521 hyperaccumulator plant *Alyssum lesbiacum*. *Biometals* **18**, 627–641
- 522 Ingram J. & Bartels D. (1996) The molecular basis of dehydration tolerance in plants. *Annual Review*
523 *of Plant Physiology and Plant Molecular Biology* **47**, 377–403
- 524 Jalink H., van der Schoor R., Frandas A., van Pijlen J.G. & Bino R.J. (1998) Chlorophyll fluorescence
525 of *Brassica oleracea* seeds as a non-destructive marker for seed maturity and seed
526 performance. *Seed Science Research* **8**, 437–443
- 527 Jovanović Ž., Rakić T., Stevanović B. & Radović S. (2011) Characterization of oxidative and
528 antioxidative events during dehydration and rehydration of resurrection plant *Ramonda*
529 *nathaliae*. *Plant Growth Regulation* **64**, 231–240

- 530 Kranner I., Beckett R.P., Wornik S., Zorn M. & Pfeifhofer H.W. (2002) Revival of a resurrection plant
531 correlates with its antioxidant status. *The Plant Journal* **31**, 13–24
- 532 Kräutler B. (2008) Chlorophyll breakdown and chlorophyll catabolites in leaves and fruit.
533 *Photochemical and Photobiological Sciences* **7**, 1114–1120
- 534 Kräutler B. & Hörtensteiner S. (2013) Chlorophyll Breakdown: Chemistry, Biochemistry and Biology.
535 In *Handbook of Porphyrin Science* (eds G.C. Ferreira, K.M. Kadish, K.M. Smith, R. Guilard),
536 Vol. 28, pp. 117–185. World Scientific Publishing, USA.
- 537 Kräutler B. & Matile P (1999) Solving the riddle of chlorophyll breakdown. *Accounts of Chemical*
538 *Research* **32**, 35–43
- 539 Moser S., Müller T., Oberhuber M. & Kräutler B. (2009) Chlorophyll catabolites - Chemical and
540 structural footprints of a fascinating biological phenomenon. *European Journal of Organic*
541 *Chemistry*, 21–31
- 542 Moser S., Aarts M., Müller T. & Kräutler B. (2008) A yellow chlorophyll catabolite is a pigment of
543 the fall colours. *Photochemical and Photobiological Sciences* **7**, 1577–1581
- 544 Mowla S.B., Thomson J.A., Farrant J.M. & Mundree S.G. (2002) A novel stress-inducible antioxidant
545 enzyme identified from the resurrection plant *Xerophyta viscosa* Baker. *Planta* **215**, 716–726
- 546 Mühlecker W., Kräutler B., Moser D., Matile P. & Hörtensteiner S. (2000) Breakdown of chlorophyll:
547 a fluorescent chlorophyll catabolite from sweet pepper (*Capsicum annuum*). *Helvetica Chimica*
548 *Acta* **83**, 278–286
- 549 Mühlecker W., Ongania K.-H., Kräutler B., Matile P. & Hörtensteiner S. (1997) Tracking down
550 chlorophyll breakdown in plants: elucidation of the constitution of a “fluorescent” chlorophyll
551 catabolite. *Angewandte Chemie International Edition* **36**, 401–404
- 552 Nakajima S., Ito H., Tanaka R. & Tanaka A. (2012) Chlorophyll *b* reductase plays an essential role in
553 maturation and storability of *Arabidopsis* seeds. *Plant Physiology* **160**, 261–273
- 554 Nelson N. & Yocum C.F. (2006) Structure and function of photosystems I and II. *Annual Review of*
555 *Plant Biology* **57**, 521–565
- 556 Oberhuber M., Berghold J., Breuker K., Hörtensteiner S. & Kräutler B. (2003) Breakdown of
557 chlorophyll: a nonenzymatic reaction accounts for the formation of the colorless

- 558 “nonfluorescent” chlorophyll catabolites. *Proceedings of the National Academy of Sciences of*
559 *the United States of America* **100**, 6910–6915
- 560 Park S.-Y., Yu J.-W., Park J.-S., *et al* (2007) The senescence-induced STAYGREEN protein regulates
561 chlorophyll degradation. *The Plant Cell* **19**, 1649–1664
- 562 Pérez P., Rabneć G., Laufer Z., Gutiérrez D., Tuba Z. & Martínez-Carrasco R. (2011) Restoration of
563 photosystem II photochemistry and carbon assimilation and related changes in chlorophyll and
564 protein contents during the rehydration of desiccated *Xerophyta scabrida* leaves. *Journal of*
565 *Experimental Botany* **62**, 895–905
- 566 Peters S., Mundree S.G., Thomson J.A., Farrant J.M. & Keller F. (2007) Protection mechanisms in the
567 resurrection plant *Xerophyta viscosa* (Baker): both sucrose and raffinose family
568 oligosaccharides (RFOs) accumulate in leaves in response to water deficit. *Journal of*
569 *Experimental Botany* **58**, 1947–1956
- 570 Proctor M.C.F. & Tuba Z. (2002) Poikilohydry and homoihydry: antithesis or spectrum of
571 possibilities? *New Phytologist* **156**, 327–349
- 572 Pružinská A., Anders I., Aubry S., Schenk N., Tapernoux-Lüthi E., Müller T., Kräutler B. &
573 Hörtensteiner S. (2007) In vivo participation of red chlorophyll catabolite reductase in
574 chlorophyll breakdown. *The Plant Cell* **19**, 369–387
- 575 Pružinská A., Anders I., Tanner G., Roca M. & Hörtensteiner S. (2003) Chlorophyll breakdown:
576 pheophorbide *a* oxygenase is a Rieske-type iron-sulfur protein, encoded by the *accelerated*
577 *cell death 1* gene. *Proceedings of the National Academy of Sciences of the United States of*
578 *America* **100**, 15259–15264
- 579 Pružinská A., Tanner G., Aubry S., *et al* (2005) Chlorophyll breakdown in senescent *Arabidopsis*
580 leaves: characterization of chlorophyll catabolites and of chlorophyll catabolic enzymes
581 involved in the degreening reaction. *Plant Physiology* **139**, 52–63
- 582 Rascio N. & Rocca N.L. (2005) Resurrection plants: the puzzle of surviving extreme vegetative
583 desiccation. *Critical Reviews in Plant Science* **24**, 209–225

- 584 Rodoni S., Mühlecker W., Anderl M., Kräutler B., Moser D., Thomas H., Matile P. & Hörtensteiner S.
 585 (1997) Chlorophyll breakdown in senescent chloroplasts. Cleavage of pheophorbide *a* in two
 586 enzymic steps. *Plant Physiology* **115**, 669-676
- 587 Sakuraba Y., Kim Y.-S., Yoo S.-C., Hörtensteiner S. & Paek N.-C. (2013) 7-Hydroxymethyl
 588 chlorophyll *a* reductase functions in metabolic channeling of chlorophyll breakdown
 589 intermediates during leaf senescence. *Biochemical and Biophysical Research Communications*
 590 **430**, 32–37
- 591 Sakuraba Y., Schelbert S., Park S.Y., Han S.H., Lee B.D., Andr  s C.B., Kessler F., Hörtensteiner S. &
 592 Paek N.-C. (2012) STAY-GREEN and chlorophyll catabolic enzymes interact at light-
 593 harvesting complex II for chlorophyll detoxification during leaf senescence in *Arabidopsis*.
 594 *The Plant Cell* **24**, 507–18
- 595 Schelbert S., Aubry S., Burla B., Agne B., Kessler F., Krupinska K. & Hörtensteiner S. (2009)
 596 Pheophytin pheophorbide hydrolase (pheophytinase) is involved in chlorophyll breakdown
 597 during leaf senescence in *Arabidopsis*. *The Plant Cell* **21**, 767–785
- 598 Scherl M., M  ller T. & Kr  utler B. (2012) Chlorophyll catabolites in senescent leaves of the lime tree
 599 (*Tilia cordata*). *Chemistry & Biodiversity* **9**, 2605-2617
- 600 Schneider K., Wells B., Schmelzer E., Salamini F. & Bartels D. (1993) Desiccation leads to the rapid
 601 accumulation of both cytosolic and chloroplastic proteins in the resurrection plant
 602 *Craterostigma plantagineum* Hochst. *Planta* **189**, 120–131
- 603 Scott P. (2000) Resurrection plants and the secrets of eternal leaf. *Annals of Botany* **85**, 159–166
- 604 Sherwin H.W. & Farrant J.M. (1996) Differences in rehydration of three desiccation-tolerant
 605 angiosperm species. *Annals of Botany* **78**, 703–710
- 606 Sherwin H.W. & Farrant J.M. (1998) Protection mechanisms against excess light in the resurrection
 607 plants *Craterostigma wilmsii* and *Xerophyta viscosa*. *Plant Growth Regulation* **24**, 203–210
- 608 Solymosi K., Tuba Z. & B  ddi B. (2013) Desiccoplast–etioplast–chloroplast transformation under
 609 rehydration of desiccated poikilochlorophyllous *Xerophyta humilis* leaves in the dark and
 610 upon subsequent illumination. *Journal of Plant Physiology* **170**, 583–590

- 611 Strain H.H., Cope B.T. & Svec W.A. (1971) Analytical procedures for the isolation, identification,
612 estimation and investigation of the chlorophylls. *Methods in Enzymology* **23**, 452–476
- 613 Süßenbacher I., Christ B., Hörtensteiner S. & Kräutler B. (2014) Hydroxymethylated phyllobilins in
614 *Arabidopsis thaliana* – a puzzling new feature of the dioxobilin-branch of chlorophyll
615 breakdown. *Chemistry - A European Journal* **20**, 87–92
- 616 Tanaka R., Hirashima M., Satoh S. & Tanaka A. (2003) The *Arabidopsis-accelerated cell death* gene
617 *ACD1* is involved in oxygenation of pheophorbide a: inhibition of pheophorbide a oxygenase
618 activity does not lead to the “stay-green” phenotype in *Arabidopsis*. *Plant and Cell Physiology*
619 **44**, 1266–1274
- 620 Tanaka R. & Tanaka A. (2011) Chlorophyll cycle regulates the construction and destruction of the
621 light-harvesting complexes. *Biochimica et Biophysica Acta* **1807**, 968–976
- 622 Thomas H. (2013) Senescence, ageing and death of the whole plant. *New Phytologist* **197**, 696–711
- 623 Thomas H., Ougham H.J., Wagstaff C. & Stead A.D. (2003) Defining senescence and death. *Journal*
624 *of Experimental Botany* **54**, 1127–1132
- 625 Toldi O., Tuba Z. & Scott P. (2009) Vegetative desiccation tolerance: is it a goldmine for
626 bioengineering crops? *Plant Science* **176**, 187–199
- 627 Tuba Z., Lichtenthaler H.K., Csintalan Z., Nagy Z. & Szente K. (1996) Loss of chlorophylls, cessation
628 of photosynthetic CO₂ assimilation and respiration in the poikilochlorophyllous plant
629 *Xerophyta scabrida* during desiccation. *Physiologia Plantarum* **96**, 383–388
- 630 Tuba Z., Lichtenthaler H.K., Csintalan Z., Nagy Z. & Szente K. (1994) Reconstitution of chlorophylls
631 and photosynthetic CO₂ assimilation upon rehydration of the desiccated poikilochlorophyllous
632 plant *Xerophyta scabrida* (Pax). *Planta* **192**, 414–420
- 633 Tuba Z., Proctor M.C.F. & Csintalan Z. (1998) Ecophysiological responses of homoiochlorophyllous
634 and poikilochlorophyllous desiccation tolerant plants: a comparison and an ecological
635 perspective. *Plant Growth Regulation* **24**, 211–217
- 636 Ulrich M., Moser S., Müller T. & Kräutler B. (2011) How the colourless “nonfluorescent” chlorophyll
637 catabolites rust. *Chemistry: A European Journal* **17**, 2330–2334

- 638 Vicré M., Farrant J.M. & Driouich A. (2004) Insights into the cellular mechanisms of desiccation
 639 tolerance among angiosperm resurrection plant species. *Plant, Cell and Environment* **27**,
 640 1329–1340
- 641 Wessel D. & Flügge U.I. (1984) A method for the quantitative recovery of protein in dilute solution in
 642 the presence of detergents and lipids. *Analytical Biochemistry* **138**, 141–143
- 643 Whittaker A., Bochicchio A., Vazzana C., Lindsey G. & Farrant J. (2001) Changes in leaf hexokinase
 644 activity and metabolite levels in response to drying in the desiccation-tolerant species
 645 *Sporobolus stapfianus* and *Xerophyta viscosa*. *Journal of Experimental Botany* **52**, 961–969
- 646 Zavaleta-Mancera H.A., Franklin K.A., Ougham H.J., Thomas H. & Scott I.M. (1999a) Regreening of
 647 senescent *Nicotiana* leaves I. Reappearance of NADPH-protochlorophyllide oxidoreductase
 648 and light-harvesting chlorophyll *a/b*-binding protein. *Journal of Experimental Botany* **50**,
 649 1677–1682
- 650 Zavaleta-Mancera H.A., Thomas B.J., Thomas H. & Scott I.M. (1999b) Regreening of senescent
 651 *Nicotiana* leaves II. Redifferentiation of plastids. *Journal of Experimental Botany* **50**, 1683–
 652 1689

653

654

655 FIGURE LEGENDS

656 **Figure 1.** Structural outline of the PAO/phyllobilin pathway of Chl breakdown. The chemical
 657 constitutions of Chl (Chl *a*, R⁰ = CH₃; Chl *b*, R⁰ = CHO) and of selected Chl catabolites are shown.
 658 Relevant carbon atoms are labeled in *p*FCC. Sites of peripheral modifications as present in DNCCs
 659 and NCCs identified from different plant species (Kräutler & Hörtensteiner 2013) are indicated (R¹ –
 660 R³). YCCs have been shown to be derived from respective NCCs by oxidation (Moser *et al.* 2008).
 661 The reactions of PAO and RCCR are indicated. Note that depending on the source of RCCR two C1
 662 stereoisomers of *p*FCC, *p*FCC or *epi-p*FCC, can be formed. Abbreviations are as indicated in the text.

663

664 **Figure 2.** RWC (a), Chl (b) content and leaf morphology (c) of *X. viscosa* leaves during dehydration (-
 665 H₂O) and rehydration (+H₂O). Data are mean values of a representative experiment with three

replicates. Error bars indicate SD. In (c), leaf morphology and color during dehydration and rehydration were imaged using a digital camera. Bar = 0.5 cm.

Figure 3. RWC (a), Chl (b) content and plant morphology (c) of *C. pumilum* leaves during dehydration (-H₂O) and rehydration (+H₂O). Four time points were assessed: "hydrated" (0 d), "partially dehydrated" (10 d), "dried" (15 d) and "rehydrated" (+ 7 d). Triangles are used to display results obtained from leaves that survived the experiment ("non-senescent") and squares refer to leaves that turned yellow and did not survive the experiment ("senescent"). Data are mean values of a representative experiment with three biological replicates. Error bars indicate SD. In (b), the significance of differences between "non-senescent" samples was determined using a two tailed t-test. In (c), leaf morphology and color during dehydration and rehydration were imaged using a digital camera. Bar = 2.0 cm.

Figure 4. Protein analyses in *X. viscosa* (a and b) and *C. pumilum* (c and d) leaves during dehydration and rehydration. (a) and (c) Total leaf protein samples corresponding to 5 mg of dry weight were separated by SDS-PAGE and stained with Coomassie blue. Rubisco (large and small subunits) are indicated with black arrowheads. (b) and (d) Immunoblot analysis of PsbA, LHCb1 and PAO levels. After SDS-PAGE as shown in panel (a) and (c), proteins were transferred onto a nitrocellulose membrane and visualized by immunoblotting using anti-PsbA, -LHCb1 and -PAO antibodies. For more details, see "Materials and Methods". Standard protein masses are given in kDa on the right.

Figure 5. Phyllobilin analyses in *X. viscosa* leaves during dehydration and rehydration. (a) Catabolites were separated using the HPLC setup "1" described in "Materials and Methods". A₂₅₄ are shown. For clarity, only the relevant parts of the HPLC traces are shown. (a) Mass and UV/Vis spectra of *Xv*-NCC-3. For more details on MS data of *Xv*-NCC-3, see "Materials and Methods". A UV/Vis spectrum of *Xv*-NCC-3 is shown in the inset. (c) HPLC co-injection of *Xv*-NCC-3 and *Zm*-NCC-2. Note that this experiment was performed with the HPLC setup "2" described in "Materials and Methods" and

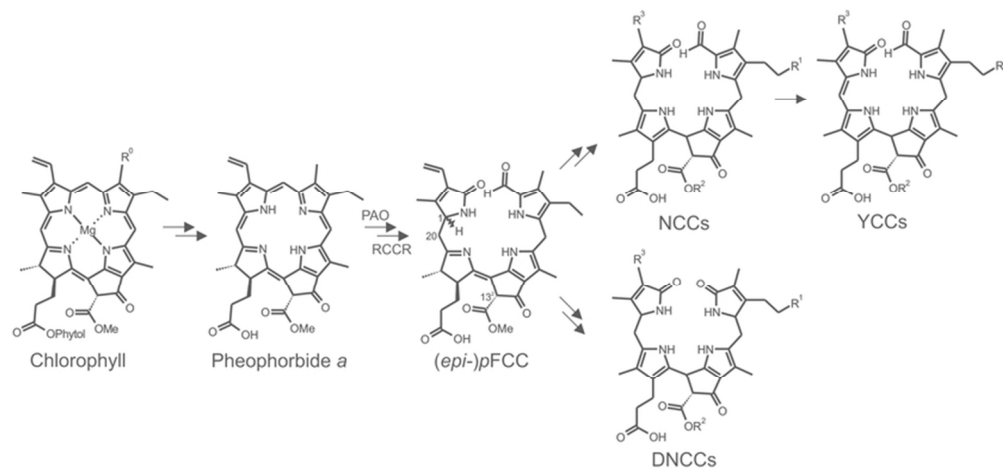
indicates that the two NCCs have the identical constitution. A_{320} are shown. (d) Chemical structure of X_V -NCC-3/ Zm -NCC-2. Relevant atoms are labeled.

Figure 6. Analysis of phyllobilins in *C. pumilum* leaves during dehydration and rehydration. (a) Catabolites were separated using the HPLC setup “1” described in "Materials and Methods". A_{254} are shown. For clarity, only the relevant parts of the HPLC traces are shown. (b) Relative amounts of NCCs and YCCs in "non-senescent" and "senescent" leaves of *C. pumilum* during dehydration and rehydration. Data are mean values of a representative experiment with three replicates and are based on equal leaf dry weight. Error bars indicate SD.

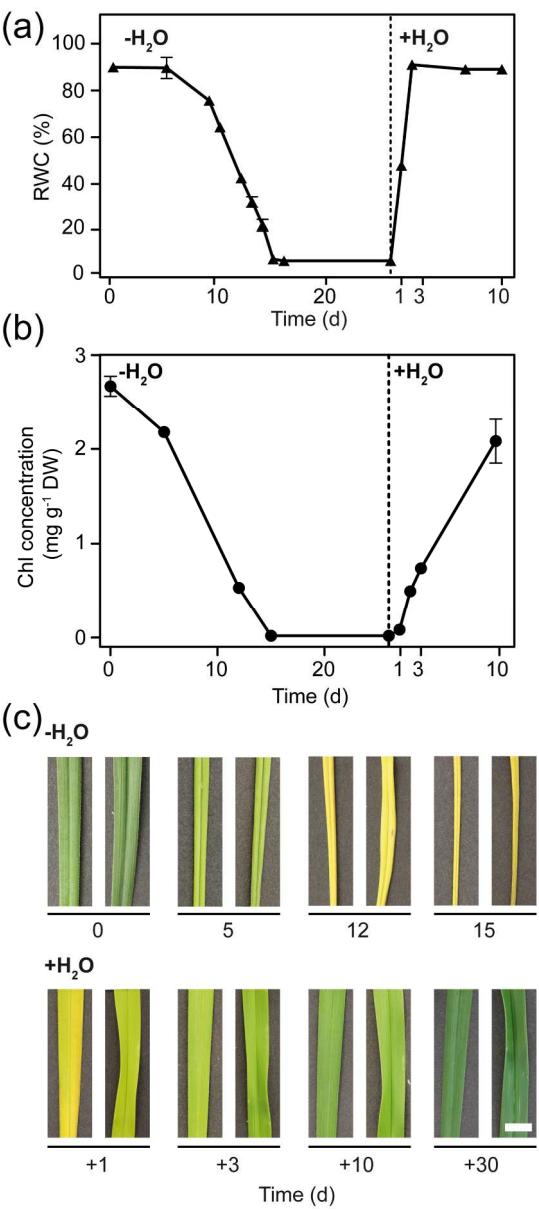
SUPPORTING INFORMATION

Additional Supporting Information may be found in the online version of this article:

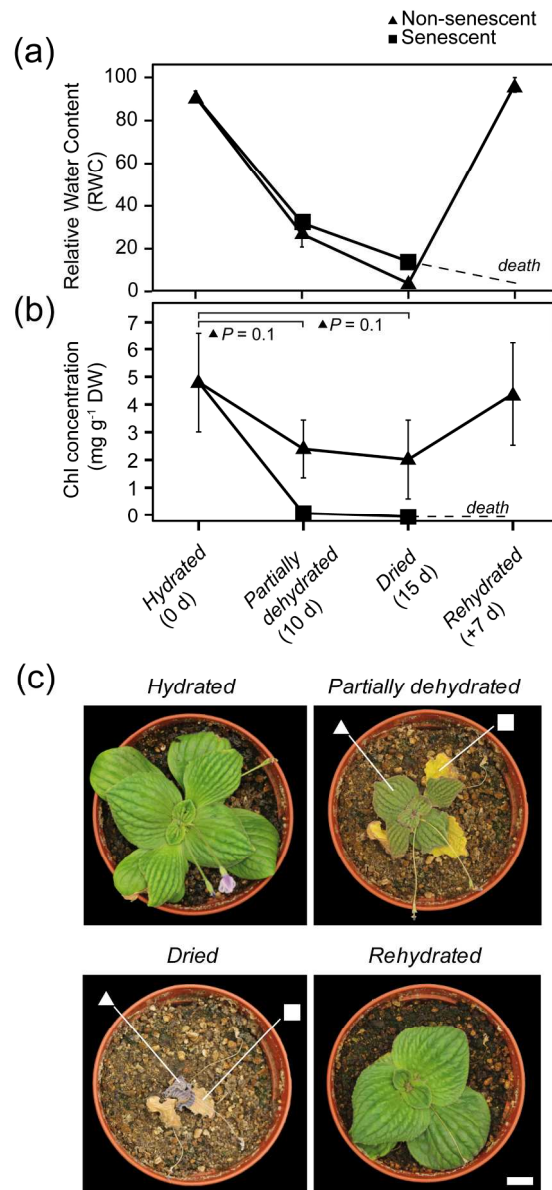
Figure S1. UV/Vis spectra of phyllobilins identified in this study.



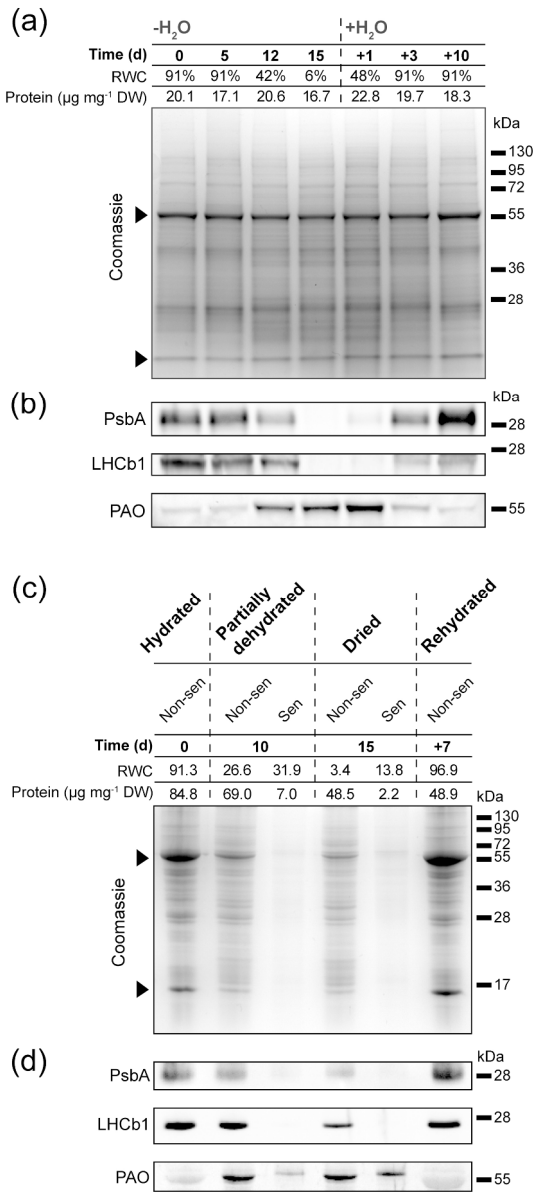
71x32mm (300 x 300 DPI)



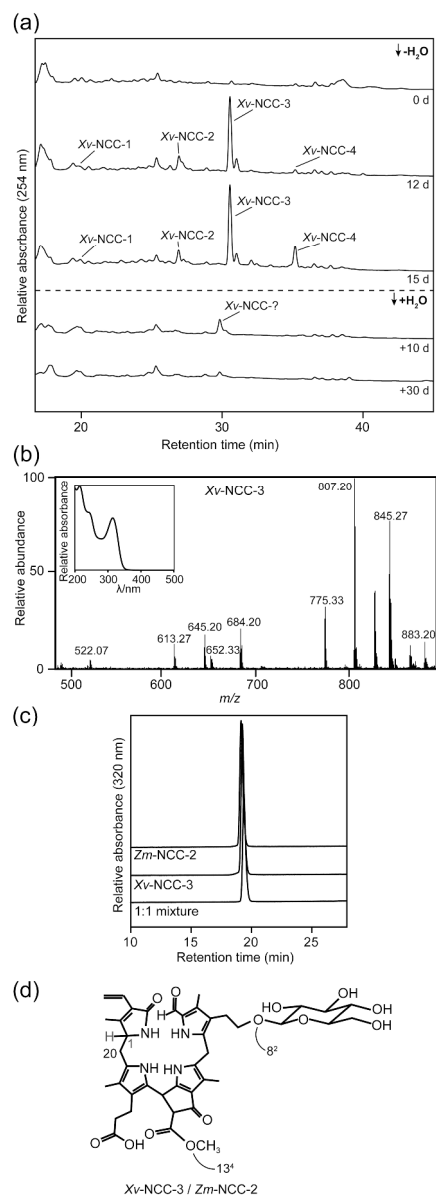
142x319mm (300 x 300 DPI)



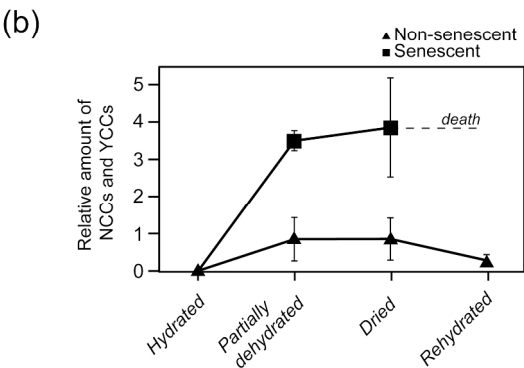
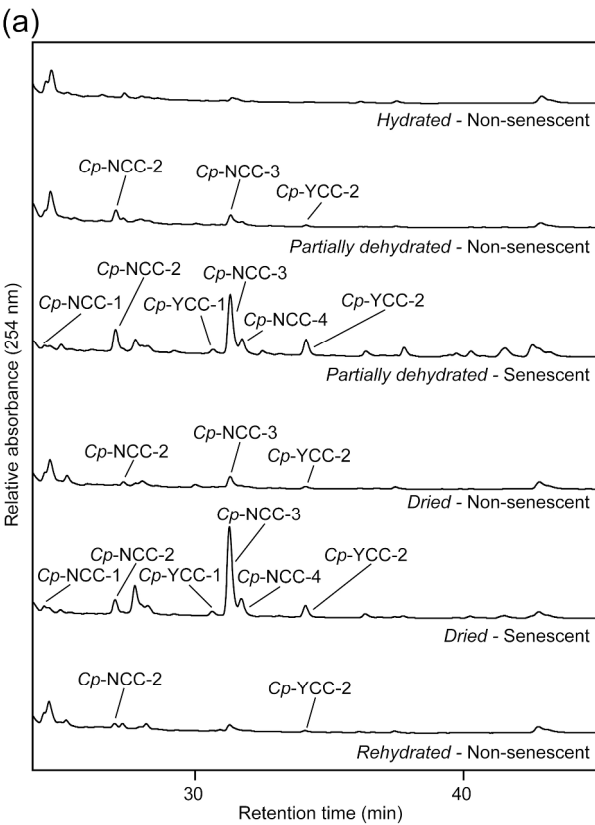
147x320mm (300 x 300 DPI)



167x374mm (300 x 300 DPI)



227x627mm (300 x 300 DPI)



162x324mm (300 x 300 DPI)

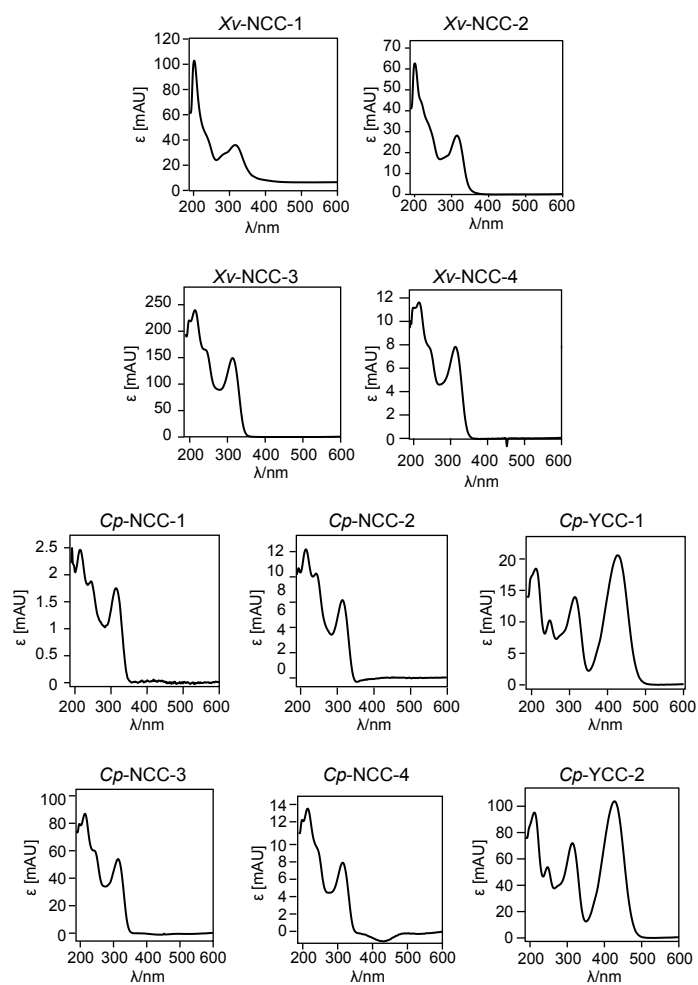


Figure S1. UV/Vis spectra of phyllobilins identified in this study